Ceramics International

Vanadium dioxide/aluminium composites for adaptive infrared stealth

Jing Wang a, Long Zeng a, Mingxu Xi a∗, Shouxun Ji b, Zhen Zhangd, Jiamiao Liang d, Weizong Bao e, Guoqiang Xie e, Jianguo Li a

a School of Materials Science and Engineering, Shanghai Jiao Tong University, Shanghai, 200240, China

b BCAST, Brunel University London, Uxbridge, UB8 3PH, United Kingdom

c Shanghai Key Lab of Advanced High-temperature Materials and Precision Forming, Shanghai Jiao Tong University, Shanghai, 200240, China

d State Key Laboratory of Metal Matrix Composites, School of Materials Science and Engineering, Shanghai Jiao Tong University, Shanghai, 200240, China

e School of Materials Science and Engineering, Harbin Institute of Technology (Shenzhen), Shenzhen, 518055, China

Keywords: Vanadium dioxide; Adaptive stealth; Low emissivity; Al-based composites

ABSTRACT

Vanadium dioxide (VO2) is assumed as a promising dynamic infrared stealth material owing to its tuneable emissivity. However , the relatively high emissivity associated with VO2 -base d adaptive infrared stealth material s poses a constraint on their practical applications. To address this issue, this proposed a VO2/ Al composite end owed with a smart infrared stealth function . With 50 % VO2 , the composite achieved a lo w emissivity value of 0.54 at 30 °C , while it exhibited a reversible variation to 0.43 at 10 0 °C , demonstrating a change up to 0.11 . When the temperature of the sample remained at 10 0 °C , the surface temperature detected by an infrared camera was only 53.4 °C , indica tin g a promising infrared stealth performance. Meanwhile, the met Al -insulator transition (MIT) effect and thermal insulation performance were investigated under the frame work of the composition effect of composite materials. The design strategy of this metal composite material paves the way for novel approaches in designing dynamic infrared stealth materials with low emissivity.

1. Introduction

The infrared stealth material s minimize the difference in infrared radiation between the target and its background through the radiation adjustment, thereby effectively evading detection and achieving stealth capabilities[1 , 2]. Achieving an effective infrared camouflage effect necessitates that stealth material s exhibit superior environmental adaptability. This is crucial because the intensity of sola r radiation , temperature , humidity, and other dynamic factors can significantly impact the infrared radiation intensity during

actual operations. However , conventional stealth materials possess a fixe d emissivity and can only conceal object s against a specific background temperature . Consequently, when the environmental condition changes, the conventional stealth material s become susceptible to re -exposure . Therefore, it is imperative to develop an intelligent material that can adapt its emissivity spontaneously to match the surrounding environment [3 – 5]. Vanadium dioxide (V O 2) has attracted much attention due to its reversible metal-insulator transition (MIT). It undergoes a phase transition from a monoclinic structure (M phase) with insulating properties to a tetragonal rutile structure (R phase) with metallic properties at the critical temperature $\tau_c \approx 68$ °C [6 , 7]. Accompanied by the phase transition , the infrared emissivity of VO2 change s significantly , from high emissivity at lo w temperature to lo w emissivity at high temperature [8 , 9]. The variable emissivity of VO2 can be used to maintain the mi n i - mu m difference between the object and the background in term s of radiation energy under a variable temperature environment, thus offering a practical approach for adaptive infrared camouflage. Moreover , the MI T temperature of VO2 can be effectively tune d through do pin g [10 –12], strain [13 ,14] and intrinsic point defect s [15 ,16]. Ji et al . demonstrate d the tunability of infrared radiation intensity of VO2 nano powders in two thermal atmospheric windows for the first time [17]. Following this , W - dope d VO2 nanoparticles were successfully pr e - pare d to reduce the transition temperature and the result s further promote the development of the adaptive camouflage [18]. Nevertheless, the emissivity of VO2 in the M phase is as high as 0. 8 –0.9, which will result in a high intensity of infrared radiation and thus not be favourable for its application in camouflage according to the infrared stealth mechanism [19].

Given the ultra-low emissivity exhibited by metals such as gold , silver, and aluminium [20 ,21], the combination of low -emissivity material s with dynamic stealth material s can be an effective strategy for enhancing infrared stealth performance. Base d on lightweight design and cost considerations, in this work , Al powders were ball milled with VO2 particles and spar k plasma sintered (SPS) to form bulk composites in order to reduce the emissivity. The impact of VO2 content on emissivity was experimentally evaluated , and the emissivity characteristics of the composites were analysed using an infrared thermal imaging camera. Furthermore , the thermal and electrical conducti vit y properties of the composites , along with their three -dimensional microstructure, were systematically investigated to explore the MI T effect and thermal insulation performance. These findings may offer valuable guidance for the development of smart infrared stealth materials with reduced emissivity.

2. Experimental

VO2 particles(99.99 wt % purity , the average size of 3 μ m) and pure Al particles(99.95 wt % purity , the average size of 25 μ m) were milled using a planetary high energy ball mill under an argon atmosphere to prepare Al -(10, 20 , 30 , 40 , 50) vol% VO2 composite powders . The ball -milling process was conducted at ambient temperature for 4 h (with a 20 mi n

interval for ever y 60 mi n milling time) at a rotation speed of 20 0 rpm, and the ball -to - powder weight ratio was 10:1 . The obtained powder was sintered at 50 0 °C for 10 mi n under an axial pressure of 50 MP a using SPS.

The microstructure of the polished samples was observed using a scanning electron microscope (SEM , Phenom XL , Phenom -World) . Energy -dispersive spectroscopy (EDS) was employed to analyse elemental mapping with an operation voltage of 15 kV . A Talos F200 X G2 transmission electron microscope (TEM) with selected area electron diffraction (SAED) was used to confirm the crystal structure . X -ray diffraction (XRD) pattern s were acquired on a Rigaku Ultima IV diffractometer (Rigaku, Japan) using Cu K α radiation (λ = 0.15 4 nm) with a scan speed of 2° /min. The electrical conductivity (σ) measurement was conducted by the standard four -probe technique in a Quantum Design Physical Property Measurement System (PPMS) . The heating and cooling rates were set at 5 °C /min. Thermal conductivities of the composites , κ , were obtained through a calculation that is equal to the product of density (ρ), heat capacity (Cp), and thermal diffusivity (D), κ = ρ·Cp·D . Here , ρ was measured using the Archimedes drainage method. Cp was determined by differential scanning calorimetry (DSC 2500 , TA). D was obtained by the lase r flash diffusivity method (LFA467, Netzsch , Germany). The infrared emissivity of the composites was investigated on the IR - 2 dual band emissivity measuring instrument (Shanghai Institute of Technical Physics, China) at the wave - length of 8 –14 μm under different temperatures. X -ray microtomography was performed on Zeiss Xradia 62 0 with a pixel size of 0. 7 μ m . The thermal images at different temperature s were taken by an infrared thermal imager working in the 8 –14 μ m region (Magnify Technologies).

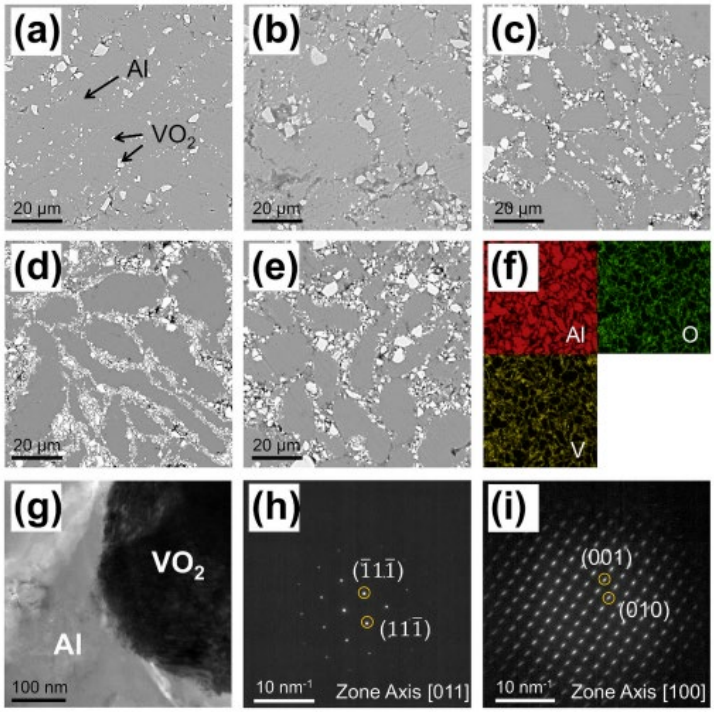

Fig. 1. (a–e) SEM images of VO2/Al composites with various VO2 contents, (a) 10 vol%, (b) 20 vol%, (c) 30 vol%, (d) 40 vol%, (e) 50 vol%, and (f) EDS mapping of the composite with 20 vol% VO2. (g) TEM image of 20 vol% VO2/Al composite and the corresponding SAED pattern of (h)Al and (i)VO2.

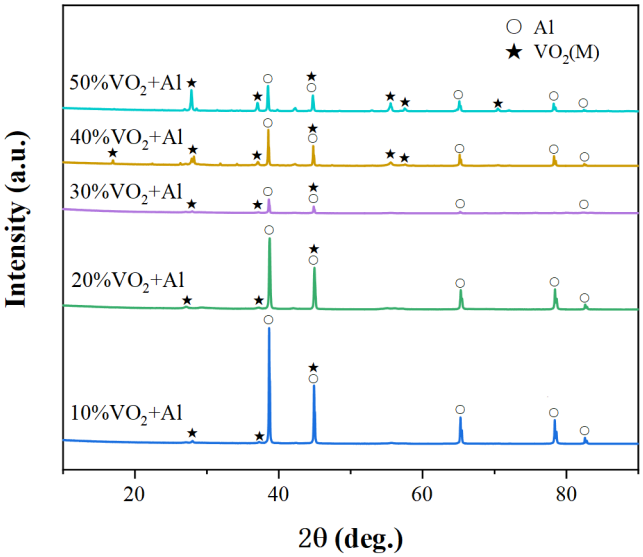

Fig. 2. XRD patterns of the VO2/Al composites with various VO2 contents.

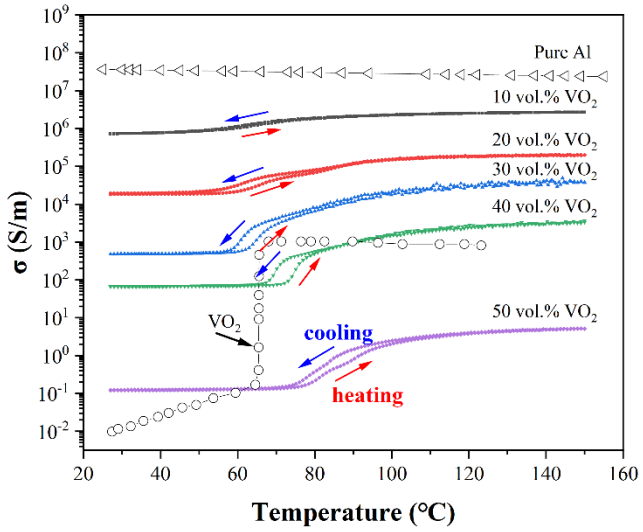

Fig. 3. Effect of temperature on the electrical conductivity of VO2/Al composites with different contents of VO2. The solid and dashed lines present data during the heating and cooling processes, respectively.

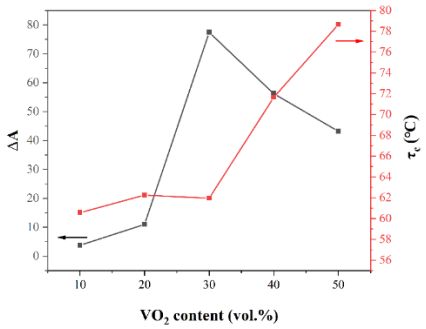

Fig. 4. Effect of VO2 contents on the electrical conductivity change (ΔA) and transition temperature (τc) of the VO2/Al composites.

3. Results

The microstructure of VO2/ Al composites with varying VO2 volumetric fraction s is depicted in Fig. 1(a –e) , while Fig. 1(f) di splays the EDS mapping for a composite containing 20 vol% VO2 . Combining with EDS results, the grey phase was pure Al, which uniformly surrounded VO2 particles in the whole picture . With the increasing volume fraction Fig. 1 . (a –e) SEM images of VO2/Al composites with various VO2 contents, (a) 10 vol% , (b) 20 vol% , (c) 30 vol% , (d) 40 vol% , (e) 50 vol% , and (f) EDS mapping of the composite with 20 vol% VO2 . (g) TEM image of 20 vol% VO2/ Al composite and the corresponding SAED pattern of (h)Al and (i) of VO2 , the bright VO2 particles aggregate d within the Al matrix and formed a VO2 network . Fig. 1(g) show s the TE M image of 20 vol% VO2/ Al composite, indica tin g the good interfacial bonding of VO2 and Al . The SAED pattern s in Fig. 1(h) and (i) revealed the well crystallization of Al and VO2 . Fig. 2 exhibits XRD pattern s of VO2/ Al composites at room temperature . The peaks of the XRD pattern s were identified according to Al (JCPDS Card No . 99 -0005) and VO2 (M) (JCPDS Card No . 43 –1051). It suggested that the obtained composites consisted of Al and VO2 (M) without any impurities.

To investigate the MIT effect of the composites , the temperature dependence of electric Al conductivity (σ) is shown in Fig. 3 . The conductivity of pure VO2 is also plotted. It can be seen that σ decrease d from 7.24 × 10 5 S/ m to 0.97 S/ m with the content of VO2 increase d from 10 vol% to 50 vol% within the lower temperature range, gradually approaching the electric Al conductivity of pure VO2 . At higher temperatures, the value of σ showed the same trend. The more the VO2 contained , the higher the increase was. The conductivity jump s were clearly presented on all samples around 68 °C . Considering the consistency of the conductivity of Al , the conductivity variation of the composite can be attributed to VO2 du e to the presence of the MIT within a similar temperature range.

In order to further identify the MI T properties of each sample, the variation of the electric Al conductivity change (ΔA) and τ c of the MI T Fig. 2 . XRD pattern s of the VO2/ Al composites with various VO2 contents. Fig. 3 . Effect of temperature on the electric Al conductivity of VO2/ Al composites with different content s of VO2 . The soli d and dashed lines present data during the heating and cooling processes, respectively . were also

calculated. The result s were plotted with respect to the VO2 contents, as shown in Fig. 4 . ΔA was defined as the ratio of conductivity at 12 0 °C and 40 °C , corresponding to the metallic phase and semiconductor phase of VO2 , respectively . It can be seen in Fig. 4 that Δ A first increase d from 3. 7 at 10 vol% VO2 to 77.4 at 30 vol% VO2 , and then decrease d to 56.2 at 40 vol% VO2 . This is because Δ A is primarily affected by two different mechanisms. First, ΔA was closely related to the VO2 content , a higher VO2 concentration led to a larger Δ A . Second, when the content of VO2 is too high , defect s such as pore s may enhance the scattering effect on electrons, leading to smaller jump s of electric Al conductivity. Therefore , there was a slight decrease in ΔA when VO2 content was 40 vol% . For 50 vol% VO2/ Al composite, ΔA was up to 3.14 orders of magnitude again, which was comparable to those reported for pure VO2 [22 ,23]. The large change of the electrical conductivity indicate d that 50 vol% VO2/ Al composite has excellent MI T behaviour. The accurate τ c can be define d from the firs t -order deviation of the conductivity variation in the heating and cooling stages . As shown in Fig. 4 , τc was increase d from 60.5 6 °C for 10 vol% VO2 to 71.7 3 °C for 50 vol% . The findings suggested that the transition temperature of the composites can be affected by manipulating the volume fraction of VO2 , which have been reported in previous studies [24 –26].

The temperature dependences of the emissivity are shown in Fig. 5 . The emissivity of pure VO2 is also characterized and shown in Fig. 5 . With the lower VO2 contents (1 0 –40 vol%), the composites showed a constant emissivity at different temperatures. In general , the emissivity of the composite is determined by the intrinsic emissivity of VO2 and Al. Sinc e the emissivity of VO2 at room temperature is much higher than that of pure Al , the emissivity of the composite increase d from 0.13 of 10 vol % to 0.28 of 40 vol% with the increase of VO2 content. The consistency of the emissivity with temperature was broken off when the addition of VO2 was increase d to 50 vol% . It revealed distinctive emissivity change s in the heating and cooling cycles indicating an inherited MIT from VO2 . A thermal hysteresis loop was also observed . It was found that the infrared emissivity could reversibly change from 0.54 at 40 °C (below τc) to 0.43 at 10 0 °C (above τ c), showing a pronounced infrared emission regulation up to 0.11. This regulation may be due to the increase in electric Al conductivity change . It was proved that the infrared emissivity of a material is inversely proportional to its electric Al conductivity [27]. The MIT temperature for emissivity change can be defined at 68.4 °C for the composite with 50 vol % VO2 , which is quite consistent with previous reports [9 ,28]. Therefore , when the VO2 content reaches as high as 50 vol% , the composite exhibits a distinct switching characteristic, and its emissivity is lower than that of pure VO2 . It provides new prospect s for the application of adaptive infrared stealth material with low emissivity.

In addition to the emissivity, the infrared stealth performance of the material is also closely relate d to the thermal conductivity [29]. According to Stefan Boltzmann' s Law, the infrared radiation intensity emanating from an object is directly proportional to its surface temperature and infrared emissivity. Therefore , low thermal conductivity can effectively

decelerate heat transfer to the surface , thereby reducing the intensity of infrared radiation . The thermal conductivity of the composite with different VO2 contents is shown in Fig. 6 . Thermal conductivity of pure Al [30] and pure VO2 [31] are also shown for comparison. Du e to the relatively lower thermal conductivity of VO2 , the thermal conductivity of the composites decrease d with the increase in VO2 content. Even with a small amount of VO2 addition, the value of the thermal conductivity dropped unexpectedly rapidly from 49.4 Wm − 1 K − 1 of 10 vol% to 12.6 Wm− 1K−1 of 20 vol% . When the volume fraction of VO2 exceeded 20 %, the VO2 network formed . The thermal conductivity was then do miniated by VO2 . It in turn showed a lower thermal conductivity of around 5 Wm − 1 K − 1 , nearly identic Al to that of pure single -crystal VO2 . Meanwhile, the thermal conductivity of the composite did not show an y obvious change across the investigated temperature range. The lo w thermal conductivity of the samples ensure s that heat cannot be rapidly transferred to the surface , thereby facilitating the application of adaptive infrared stealth materials.

In order to further evaluate the infrared radiation properties of the VO2/ Al composites , thermal images were take n in the 8 –14 μm band using an infrared camera. The imaging system is illustrated in Fig. 7(a). The bulk 50 vol% VO2/ Al composite and pure VO2 that were used for the measurement were both 1 mm in thickness and had similar surface morphology. Samples were equilibrated for at least 5 mi n at each temperature before data collection. The thermal infrared images of 50 vol% VO2/ Al composite and pure VO2 are presented in Fig. 7(b), illustrating the correlation between the radiation temperature captured by the infrared camera and the real temperature . As shown in Fig. 7(b), when the real temperature reached 30 °C , which was below τc , the radiation temperature s of 50 vol% VO2/ Al composite and VO2 were 17.7 °C and 27.3 °C , respectively , with a radiation temperature difference of 9. 6 °C . When the real temperature was raised to 10 0 °C , which was higher than τ c , the radian t temperature difference was 14.1 °C . Variation of the infrared radiation temperature of bulk 50 vol% VO2/ Al and pure VO2 at different real temperature s is shown in Fig. 7(c). The radiation temperature of the 50 vol% VO2/ Al and pure VO2 increase d li nearly with the increase in the real temperature before τ c . However , the radiation temperature of both samples changed significantly after the phase transition . The results show that the 50 vol% VO2/ Al composite effectively reduces the thermal emissivity of pure VO2 and has excellent adaptive infrared stealth performance.

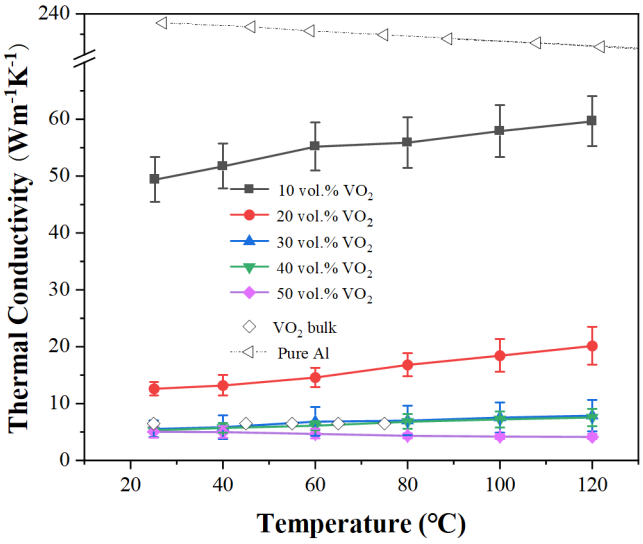

Fig. 6. Effect of temperature on the thermal conductivity of VO2/Al composites with various VO2 contents.

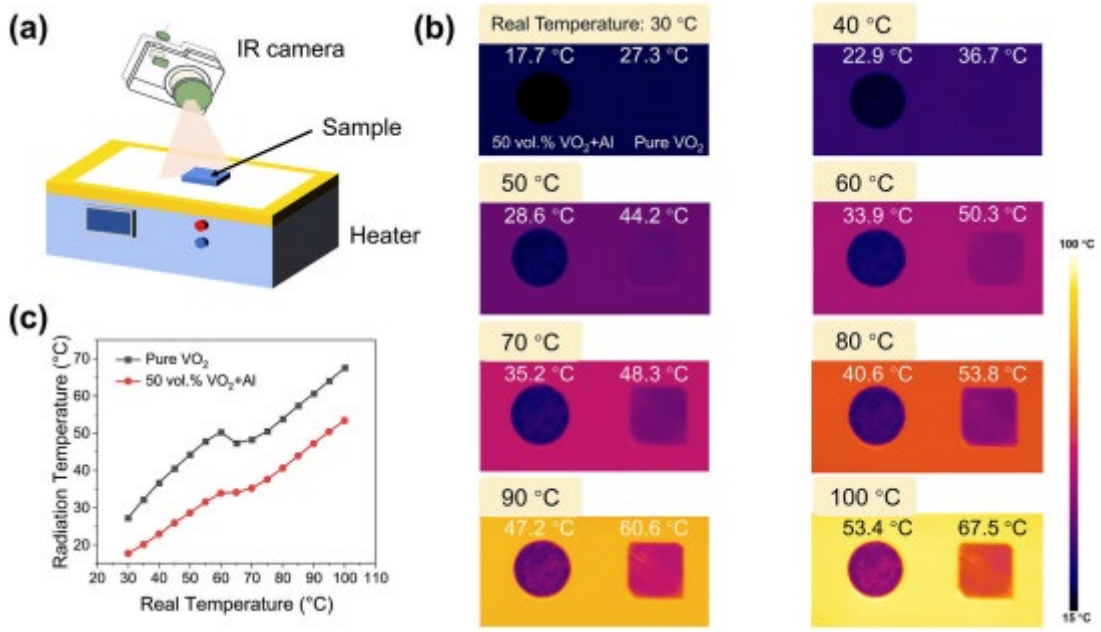

Fig. 7. (a) Schematic diagram of the infrared thermography process. (b) The infrared thermal images of the bulk 50 vol% VO2/Al composite and pure VO2 at different real temperatures. (c) The variation of radiation temperatures of bulk 50 vol% VO2/Al composite and pure VO2 as a function of real temperature.

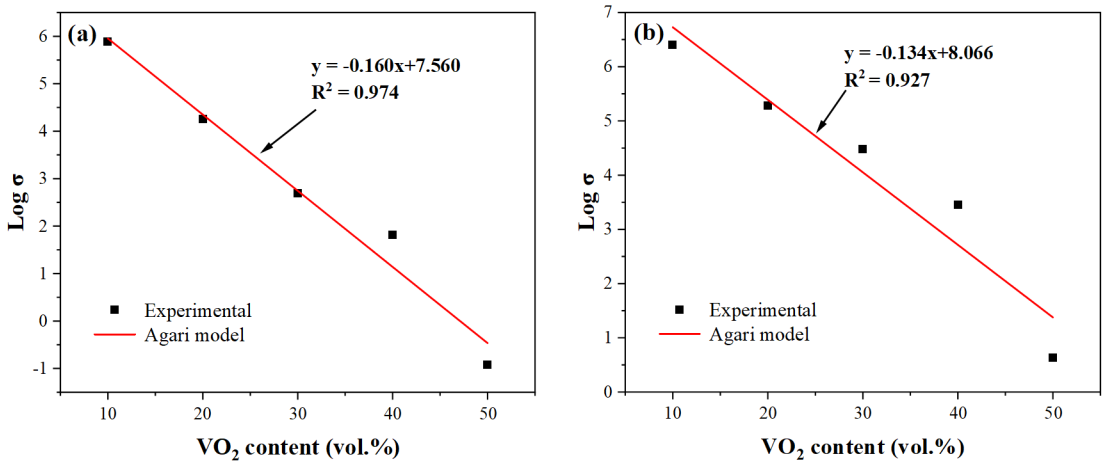

Fig. 8. Agari model fitted with experimental results of the electrical conductivity for VO2/Al composites as a function of the VO2 volume fraction at (a) 40 ◦C and (b) 120 ◦C, respectively.

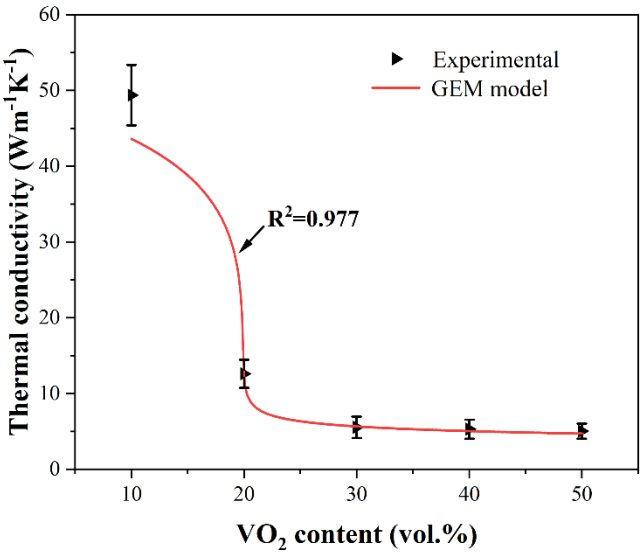

Fig. 9. Comparison of theoretically predicted thermal conductivity values by the GEM model with experimental results of VO2/Al composites as a function of the VO2 volume fraction at 25 ◦C.

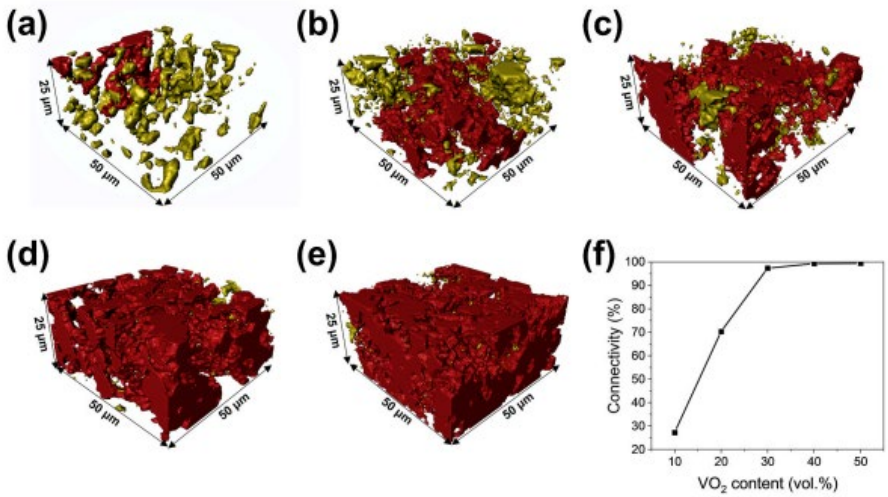

Fig. 10. Three-dimensional morphology of the VO2 particles in the composites with various VO2 contents: (a) 10 vol%, (b) 20 vol%, (c) 30 vol%, (d) 40 vol%, (e) 50 vol%, where red and yellow represent the connected and disconnected VO2 phases, respectively. (f) Effect of VO2 content on its connectivity. (For interpretation of the references to colour in this figure legend, the reader is referred to the Web version of this article.)

4 . Discussion

4. 1 . Agaric model for electrical conductivity

The abrupt change in the emissivity of the composite promises a potential infrared stealth material for smart devices. It is well known that the electrical and thermal conductivity of a material are important factors affecting its thermal stealth performance. Therefore , it is of great significance to explore the VO2 content effect on the electrical conductivity and thermal insulation performance of the VO2/ Al composite. The Agari mode l was first proposed in 1986 to explain the li near relationship between the logarithm of thermal conductivity and the volume contents of particles in composites [32]. Note that al l the data points of electrical conductivity change with VO2 content are approximately on a straight line , the experimental data can be used to fit the Agari equation in the form of electrical conductivity, as follows :

$$\log \sigma = V \bullet C2 \bullet \log \sigma 2 + (1\text{-}V) \bullet \log(C1 \bullet \sigma 1) \quad (1)$$

where σ stands for the electrical conductivity of the composite, σ 1 is the electrical conductivity of material 1 (Al in the present study) , and σ2 is the electrical conductivity of material 2 (V O 2 in the present study) . V is the volume content of material 2. C 1 is a coefficient of the effect on crystallinity and crystal size of material 1, and C2 is a coefficient of ease in forming conductive chains of material 2 [33].

As shown in Fig. 8(a) and (b), the equation fits well with the experimental results. (The data required in the mode l are obtained according to the literature [34 ,35].) Value s of coefficients C 1 and C2 in Eq . (1) are 2.10 8 and − 11.78 7 at 40 °C , 1.43 2 and 2.32 1 at

120 °C . A larger value of C1 indicate s a greater effect of VO2 particles on the electrical conductivity of Al . It seems reasonable to speculate that the VO2 particles may influence Al and alter the electrical conductivity of composites at lower temperatures because of the large difference in electrical conductivity between M -phase VO2 and Al . While at the higher temperature of 120 °C , the value of C2 become s higher . It suggests that VO2 particles are more prone to forming conductive chains at 12 0 °C (above τ c) than at 40 °C (below τ c). This phenomenon ma y be attributed to the metallic state of VO2 at 12 0 °C , characterized by higher conductivity.

4. 2 . GEM mode l for thermal conductivity and the VO2 network configuration

The general effective media (GEM) equation combines the percolation theory and the effective medium theory to construct a quantitative model, which is widely used in the electrical conductivity, thermal conductivity, particle diffusion , etc. of two -phase composites [36 –38]:

$$\frac{v_1\left(\kappa_1^{1/t}-\kappa^{1/t}\right)}{\kappa_1^{1/t}+[f_c/(1-f_c)]\kappa^{1/t}}+\frac{v_2\left(\kappa_2^{1/t}-\kappa^{1/t}\right)}{\kappa_2^{1/t}+[f_c/(1-f_c)]\kappa^{1/t}}=0 \quad (2)$$

where v1 stands for the volume fraction of the lo w -conductivity component, and v2 stands for the volume fraction of the high - conductivity component. Similarly, κ 1 and κ 2 denote the thermal conductivities of the lo w - and high -conductivity components, respectively . κ represent s the thermal conductivity of the composites . fc is a parameter relate d to the critical volume fraction for the lo w -conductivity phase, and t is an exponent.

The relationship between thermal conductivity and VO2 content at room temperature is fitted using the GE M equation . The result is shown in Fig. 9. (The data required in the model are obtained according to the literature [31 ,34 ,39].) The model predictions are in good agreement with the measured values. The derive d mode l parameters for the co m - po site include a critical volume fraction (fc) of VO2 of 0. 2 and a critic exponent (t) of 0.167. The computed percolation threshold indicate s a shar p decrease in thermal conductivity when the volume fraction of VO2 is about 20 %, which suggest s that VO2 particles form effective conductive networks in the composites . Therefore , the conduction through Al is impeded. Beyond the percolation threshold, the thermal conductivity stabilizes, approaching that of VO2 , suggesting that VO2 dominates thermal transport in this region.

In our experiment, at lower VO2 content , the discrete distribution of VO2 particles within the pure Al matrix suggests that the continuity of pure Al offers a bypass rout e for the movement of the electron s and phonons. With a high content of VO2 particles, a continuous VO2 net - work forms, which interferes with the movement s of electrons and phonons. To further prove this hypothesis, a 3D configuration of VO2 particles in the

composite was investigated using micro -CT analysis on the Zeiss Xradia 620 Versa device . As shown in Fig. 10 , when the volume fraction of VO2 is 10 %, most of the VO2 particles are isolated from each other and the connectivity is only 27.2 9 %. Therefore , the transport of electrons and phonons must go through the interaction of both Fig. 8 . Agari mode l fitted with experimental result s of the electrical conductivity for VO2/ Al composites as a function of the VO2 volume fraction at (a) 40 °C and (b) 12 0 °C , respectively . The conductivities are thus dominated by Al ne works. However , when the VO2 content is 20 vol% or higher , the conductivities are tune d by VO2 connections because the VO2 connectivity in - crease s rapidly at 20 vol% to 70.3 2 % and then reaches equilibrium when the VO2 content is 30 vol% . The results further elucidate that the thermal conductivity of the composite depends on the formation of VO2 conductive chains , confirmed by the GEM model, and its percolation threshold is 20 %.

5 . Conclusions

In the present study, VO2/ Al composites with adaptive infrared stealth properties were successfully prepared by ball milling and SPS. The VO2 content had an important effect on the stealth performance of the composite. When the amount of VO2 was 50 vol% , the emissivity of the composite varied with increasing temperature , from 0.54 to 0.43 with an emittance variability of 0.11 . The result s of the infrared thermal images showed that compared with pure VO2 , the radiation temperature of the 50 vol% VO2/ Al composite decreased by 9. 6 °C and 14.1 °C before and after the phase transition . Moreover , the lo w thermal conductivity of the composites indicated that they have good thermal insulation performance. In addition , the variation of electrical and thermal conductivities of the composites with VO2 content was investigate d to reveal the transport mechanism . It is shown that the thermal and electrical transport were consistent with the GE M mode l and the Agaric model respectively . This VO2/ Al compo sit e exhibits broad application prospects in the fields of adaptive infrared ca moulage with low emissivity.

Authorship contribution statemen t

Jing Wang : Data acquisition, Formal analysis, Investigation , Validation , Writing – original draft. Long Zeng : Funding acquisition , Re - sources, Supervision , Writing – review & editing. Mingxu Xia: Funding acquisition , Methodology, Project administration , Supervision , Writing – review & editing. Shouxun Ji : Supervision , Writing – review & editing. Zhen Zhang: Methodology, Resources. Jiamiao Liang: Investigation , Resources. Weizon g Bao: Resources, Supervision . Guoqiang Xie: Form Al analysis, Resources, Supervision . Jianguo Li: Funding acquisition , Project administration , Resources, Software . Declaration of competing interest The authors declare that they have no know n competing financial interests or personal relationship s that could have appeared to influence the work reported in this paper.

Acknowledgements

This work was supported by the National Ke y Research and Development Program s – Intergovernmental International Scientific and Technological Innovation and Cooperation Program (2022YFE0138000), National Natural Science Foundation of Chin a (E516 0 4173).

References

[1] R . Hu , W . Xi , Y . Li u , K . Tang , J . Song , X . Lu o , J . Wu , C . - W . Qi u , Thermal camouflaging metamaterial s , Mater. Toda y 45 (2021) 12 0 –14 1 , https://doi.org/ 10.1016/j.mattod.2020.11.013 .

[2] J . Hu , Y . Hu , Y . Ye , R . Shen , Unique applications of carbon material s in infrared stealth: a review , Chem . Eng. J. 45 2 (2023) 139147 , https://doi.org/10.1016/ j.cej.2022.13914 7 .

[3] L . Xiao , H . Ma , J . Li u , W . Zhao , Y . Ji a , Q . Zhao , K . Li u , Y . Wu , Y . We i , S . Fa n , K . Jian g , Fast adaptive thermal camouflage base d on flexible VO2 /graphene /CN T thin film s , Nano Lett . 15 (2015) 8365 –8370 , https://doi.org/10.1021/ acs.nanolett.5b04090 .

[4] O . Salihogl u , H . B . Uzlu , O . Yaka r , S . Aa s , O . Balc i , N . Kakeno v , S . Balc i , S . Olcu m , S . Süze r , C . Kocaba s , Graphene -base d adaptive thermal camouflage , Nano Lett . 18 (2018) 4541 –4548 , https://doi.org/10.1021/acs.nanolett.8b01746 .

[5] M . Li , D . Li u , H . Chen g , L . Peng , M . Zu , Manipulating metals for adaptive thermal camouflage , Sci. Adv. 6 (2020) https://doi.org/10.1126/sciadv.aba3494 , eaba3494 .

[6] F . J . Mori n , Oxides whic h show a met Al -to -insulator transition at the Neel temperatur e , Phys . Rev. Lett . 3 (1959) 34 –36 , https://doi.org/10.1103/ PhysRevLett.3.34 .

[7] K . Li u , S . Le e , S . Yang , O . Delair e , J . Wu , Recent progresses on physic s and applications of vanadium dioxid e , Mater. Toda y 21 (2018) 87 5 –89 6 , https:// doi.org/10.1016/j.mattod.2018.03.029 .

[8] X . Ao , B . Li , B . Zhao , M . Hu , H . Re n , H . Yang , J . Li u , J . Ca o , J . Feng , Y . Yang , Z . Qi , L . Li , C . Zo u , G . Pe i , Self-adaptive integratio n of photothermal and radiativ e coolin g for continuous energy harvesting from the su n and oute r spac e , Proc . Natl . Acad . Sci. U.S.A. 11 9 (2022) e212055711 9 , https://doi.org/10.1073/ pnas.212055711 9 .

[9] D . Li u , H . Chen g , X . Xing , C . Zhan g , W . Zhen g , Thermochromi c properties of W - dope d VO2 thin film s deposite d by aqueou s so l -ge l method for adaptive infrared stealth applicatio n , Infrared Phys . Technol. 77 (2016) 33 9 –34 3 , https://doi.org/ 10.1016/j.infrared.2016.06.019 .

[10] N . Suzuki , Y . Xu e , T . Hasegawa , S . Yi n , Phas e transition behavior and optic Al properties of F/Mo co -dope d VO2 for smart window s , Sol. Energy Mater. Sol. Cell s 25 1 (2023) 112105 , https://doi.org/10.1016/j.solmat.2022.112105 .

[11] D . Li , Z . Zhao , C . Wang , S . Deng , J . Yang , X . Wang , J . Li , Y . Zhao , H . Ji n , Influenc e of the charge compensation effect on the met Al –insulator transition of Mg - W co -dope d VO2 , Appl . Surf. Sci. 57 9 (2022) 151990 , https://doi.org/10.1016/ j.apsusc.2021.151990 .

[12] Q . Zhou , W . Lv , Q . Qi u , T . Zhou , C . Huan g , L . Li , Boro n dope d M -phas e VO2 nanoparticle s with lo w met Al -insulator phas e transition temperatur e for smart window s , Ceram. Int. 46 (2020) 4786 –4794 , https://doi.org/10.1016/ j.ceramint.2019.10.211 .

[13] J . Ca o , E . Erteki n , V . Srinivasan , W . Fa n , S . Huan g , H . Zhen g , J . W . Yi m , D . R . Khanal , D . F . Ogletree , J . C . Grossman , J . Wu , Strain engineerin g and on e - dimension Al organization of met Al -insulator domain s in single -cryst Al vanadium dioxid e beam s , Nat. Nanotechnol. 4 (2009) 73 2 –73 7 , https://doi.org/10.1038/ nnano.2009.266 .

[14] Y . Muraok a , Z . Hiro i , Met Al –insulator transition of VO2 thin film s grow n on Ti O 2 (001) and (110) substrates , Appl . Phys . Lett . 80 (2002) 58 3 –58 5 , https://doi.org/ 10.1063/1.144621 5 .

[15] S . Zhan g , I . S . Ki m , L . J . Lauhon , Stoichiometr y engineerin g of monoclinic to rutile phas e transition in suspende d single crystallin e vanadium dioxid e nanobeam s , Nano Lett . 11 (2011) 1443 –1447 , https://doi.org/10.1021/nl103925 m .

[16] J . Jeon g , N . Aetukuri , T . Graf, T . D . Schlad t , M . G . Samant , S . S . Parkin , Suppressio n of met Al -insulator transition in VO2 by electric fiel d -induce d oxygen vacanc y formatio n , Scienc e 33 9 (2013) 1402 –1405 , https://doi.org/10.1126/ science.123051 2 .

[17] H . Ji , D . Li u , H . Chen g , C . Zhan g , L . Yang , Vanadium dioxid e nanopowder s with tunabl e emissivity for adaptive infrared camouflage in both thermal atmospheri c window s , Sol. Energy Mater. Sol. Cell s 17 5 (2018) 96 –10 1 , https://doi.org/ 10.1016/j.solmat.2017.10.013 .

[18] H . Ji , D . Li u , H . Chen g , Infrared optic Al modulation characteristic s of W -dope d VO2 (M) nanoparticle s in the MWIR and LWIR region s , Mater. Sci. Semicond . Process. 11 9 (2020) 105141 , https://doi.org/10.1016/j.mssp.2020.105141 .

[19] L . Peng , D . Li u , H . Chen g , S . Zhou , M . Zu , A multilayer film base d selectiv e thermal emitte r for infrared stealth technology , Adv. Opt. Mater. 6 (2018) 180100 6 , https://doi.org/10.1002/adom.201801006 .

[20] K . Wang , C . Wang , Y . Yi n , K . Chen , Modification of Al pigmen t with graphene for infrared /visual stealth compatible fabric coatin g , J. Alloys Compd. 69 0 (2017) 74 1 –74 8 , https://doi.org/10.1016/j.jallcom.2016.08.17 1 .

[21] X . Ya n , G . Xu , Corrosio n and mechanical properties of polyurethane /Al composit e coatings with lo w infrared emissivity , J. Alloys Compd. 49 1 (2010) 64 9 –65 3 , https://doi.org/10.1016/j.jallcom.2009.11.03 0 .

[22] D . Brassard , S . Fourmaux , M . Jean -Jacque s , J . C . Kieffe r , M . A . El Khakan i , Grai n size effect on the semiconducto r -met Al phas e transition characteristic s of magnetro n -sputtere d VO2 thin film s , Appl . Phys . Lett . 87 (2005) 051910 , https:// doi.org/10.1063/1.200113 9 .

[23] J . - L . Victor , M . Gaudon , N . Peni n , A . Chiron , U . C . Chun g , O . Viraphon g , A . Rougie r , Innovative sinterin g proces s for fabricatio n of thermochromi c smooth VO2 ceramics , J. Alloys Compd. 89 0 (2022) 161890 , https://doi.org/10.1016/ j.jallcom.2021.16189 0 .

[24] B . Chen , D . Yang , P . A . Charpentie r , M . Zema n , Al3+ -dope d vanadium dioxid e thin film s deposite d by PL D , Sol. Energy Mater. Sol. Cell s 93 (2009) 1550 –1554 , https://doi.org/10.1016/j.solmat.2009.04.005 .

[25] C . Ji , Z . Wu , X . Wu , J . Wang , J . Go u , Z . Huan g , H . Zhou , W . Ya o , Y . Jian g , Al -dope d VO2 film s as smart window coatings : reduce d phas e transition temperatur e and improved thermochromi c performanc e , Sol. Energy Mater. Sol. Cell s 17 6 (2018) 17 4 –18 0 , https://doi.org/10.1016/j.solmat.2017.11.026 .

[26] A . Gentle , G . B . Smit h , Dual met Al –insulator and insulator –insulator switchin g in nanoscal e and Al dope d VO2 , J. Phys . D Appl . Phys . 41 (2008) 015402 , https:// doi.org/10.1088/0022 -3727 /41 /1/015402 .

[27] H . Yu , G . Xu , X . Shen , X . Ya n , C . Chen g , Lo w infrared emissivity of polyurethane / Cu composit e coatings , Appl . Surf. Sci. 25 5 (2009) 6077 –6081 , https://doi.org/ 10.1016/j.apsusc.2009.01.019 .

[28] Z . Ma o , W . Wang , Y . Li u , L . Zhan g , H . Xu , Y . Zhon g , Infrared stealth property base d on semiconducto r (M) -to -metallic (R) phas e transition characteristic s of W - dope d VO2 thin film s coated on cotton fabric s , Thin Soli d Film s 55 8 (2014) 20 8 –21 4 , https://doi.org/10.1016/j.tsf.2014.02.05 5 .

[29] Z . Ha n , Y . Shen , C . Li , R . Chen , J . Li , S . Gu o , Enhancemen t of infrared stealth performanc e of ultr a -high molecula r weight polyethylene -base d composites through the multilayer structural construction , Compos . Sci. Technol. 24 1 (2023) 110150 , https://doi.org/10.1016/j.compscitech.2023.11015 0 .

[30] S . Aksö z , Y . Ocak , N . Maraşl ı , E . Çadirl i , H . Kaya , U . Böyü k , Dependency of the thermal and electrical conductivity on the temperatur e and compositio n of Cu in the Al base d Al -Cu alloys , Exp. Therm. Flui d Sci. 34 (2010) 1507 –1516 , https:// doi.org/10.1016/j.expthermflusci.2010.07.015 .

[31] C . N . Berglund , H . J . Guggenheim , Electronic properties of VO2 near the semiconducto r -met Al transition , Phys . Rev. 18 5 (1969) 1022 –1033 , https:// doi.org/10.1103/PhysRev.185.1022 .

[32] Y . Agar i , T . Un o , Estimation on thermal conductivities of filled polymers , J. Appl . Polym. Sci. 32 (1986) 5705 –5712 , https://doi.org/10.1002/app.1986.070320702 .

[33] Y . Agar i , A . Ueda , M . Tanaka , Thermal conductivity of a polyme r filled with particle s in the wide rang e from lo w to supe r high volume conten t , J. Appl . Polym. Sci. 40 (1990) 92 9 –94 1 , https://doi.org/10.1002/app.1990.070400526 . [34] J . Molina , R . Prieto , J . Narcis o , E . Loui s , The effect of porosity on the thermal conductivity of Al –12wt.% Si /Si C composites , Scr. Mater. 60 (2009) 58 2 –58 5 , https://doi.org/10.1016/j.scriptamat.2008.12.015 .

[35] G . J . Hyland , On the electronic phas e transition s in the lowe r oxides of vanadium , J. Phys . C Soli d Stat e Phys . 1 (1968) 18 9 –20 7 , https://doi.org/10.1088/0022 - 3719 /1/1/32 2 .

[36] D . S . McLachla n , M . Blaszkiewicz , R . E . Newnha m , Electrical resistivit y of composites , J. Am . Ceram. Soc. 73 (1990) 2187 –2203 , https://doi.org/10.1111/ j.1151 - 2916.1990.tb07576. x .

[37] N . Deprez , D . S . McLachla n , I . Sigala s , The measuremen t and comparativ e analysis of the electrical and thermal conductivities , permeability and Youn g ’ s modulu s of sintered nickel , Soli d Stat e Commun . 66 (1988) 86 9 –87 2 , https:// doi.org/10.1016/0038 - 1098(88)9040 3 - 6 .

[38] D . S . McLachla n , An equation for the conductivity of binary mixtures with anisotropi c grai n structures , J. Phys . C Soli d Stat e Phys . 20 (1987) 86 5 –87 7 , https://doi.org/10.1088/0022 -3719 /20 /7/004/meta .

[39] N . Stojanovic , D . H . S . Maithripal a , J . M . Berg , M . Holt z , Thermal conductivity in metallic nanostructures at high temperature: electrons, phonons, and the Wiedeman n -Fran z la w , Phys . Rev. B 82 (2010) 075418 , https://doi.org/10.1103/ PhysRevB.82.075418 . 7